
VISUAL PRIVACY PROTECTION BASED ON TYPE-I ADVERSARIAL ATTACK

Zhigang Su
Xidian University

Dawei Zhou
Xidian University

Decheng Liu
Xidian University

Nannan Wang *
Xidian University

Zhen Wang
Zhejiang Lab

Xinbo Gao
Chongqing University of
Posts and Telecommunications

ABSTRACT

With the development of online artificial intelligence systems, many deep neural networks (DNNs) have been deployed in cloud environments. In practical applications, developers or users need to provide their private data to DNNs, such as faces. However, data transmitted and stored in the cloud is insecure and at risk of privacy leakage. In this work, inspired by Type-I adversarial attack, we propose an adversarial attack-based method to protect visual privacy of data. Specifically, the method encrypts the visual information of private data while maintaining them correctly predicted by DNNs, without modifying the model parameters. The empirical results on face recognition tasks show that the proposed method can deeply hide the visual information in face images and hardly affect the accuracy of the recognition models. In addition, we further extend the method to classification tasks and also achieve state-of-the-art performance.

1 Introduction

In recent years, deep neural networks (DNNs) have been deeply researched and achieved great achievements. To enable DNN-based artificial intelligence systems to provide extensive and convenient services, more and more DNNs are deployed in cloud environments, bringing efficient access to various users. This requires developers or users to upload their private data to DNNs in the cloud. However, the cloud environments are typically untrustworthy [1], with problems such as data leakage and identity theft [2]. Therefore, how to effectively protect the private information in the cloud has always been a common concern [3, 4, 5]. In this paper, we mainly focus on the visual privacy protection, which is crucial and urgent in the real world.

There are two classic types of methods suitable for visual privacy protection in the cloud environments [6]: homomorphic encryption (HE)-based methods [7, 8, 9] and perceptual encryption (PE)-based methods [10, 6, 11, 12, 13]. However, affected by the nonlinear activation functions in DNNs, HE-based methods are difficult to perform well on advanced DNNs [6]. Although PE-based methods are applicable to DNNs, existing methods typically require retraining with data in the encrypted domain to guarantee accuracy on encrypted data [10, 6]. This results in interferes with the performance on the original data and additional resource consumption (especially for large models).

To alleviate these negative affects, we expect to protect visual privacy without making any modifications to DNNs in the cloud. Namely, we hide sensitive visual information only by varying the input data. Previous researches have made some explorations in this regard. The transformation network-based methods [13], which try to encrypt the original data via a transformation function parameterized by a neural network, share the same philosophy. However, the method cannot easily recover original data from encrypted data for other purposes, and they may suffer from adversarial vulnerability [14, 15] because the introduced neural network may be destroyed by adversarial attacks.

In fact, the negative effects of adversarial attacks can be utilized positively to protect privacy. Some works have exploited adversarial attacks for de-identification [16, 17, 18]. These methods add imperceptible perturbations or

*preprint. Corresponding to nmwang@xidian.edu.cn.

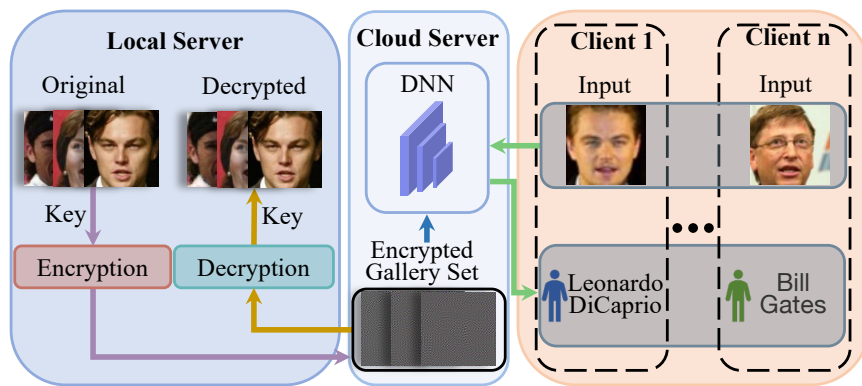


Figure 1: Illustration of the visual privacy protection. Take face recognition as an example. The gallery set is encrypted and provided to the DNN in the cloud. Encrypted data has quite different visual information with original data, but it is still correctly identified. The encrypted gallery set can be recovered by a key model by the owner.

non-suspicious patches generated by adversarial attacks to original images, hindering DNNs to extract effective features and recognize identities, thus protecting the identity privacy in the data. However, in this work, we focus on protecting visual information, which means that the protected data is completely different from the original data visually but can still be correctly predicted by DNNs (see Fig. 1). Fortunately, we observe a special type of adversarial attacks (called Type-I attack) that is significantly different from the type used in previous methods [19]. This type of attacks guides DNNs to make consistent predictions on two quite distinct samples, thus can be naturally applied to visual privacy protection.

Inspired by Type-I attacks, in this paper, we propose an *adversarial attack-based visual privacy protection (AVP)* method. The proposed method encrypts the original data while preserving its functional features for DNNs (*e.g.*, recognition features and classification features), and it can recover original samples from encrypted data for their owners. Specifically, we reduce the visual correlation between encrypted data and original data while minimizing their distance in the feature space of DNNs, to generate the encrypted data. Meanwhile, we exploit a generative model pre-trained in a private training setting as the key model, and optimize the encrypted data based on it so that the recovered data is similar to the original data. Furthermore, to break through the tough trade-off between the capability of privacy protection and the quality of restored data, we design the variance consistency loss to enhance privacy protection without compromising data recovery (see Sec. 3.3). Note that the encrypted data generated by the proposed method can only be accurately recovered by the own key model, other models (even if the model architecture is the same) are difficult to recover them well (see Sec. 4.3).

To demonstrate the effectiveness of the proposed method, we conduct comprehensive experiments on face recognition tasks and classification tasks. For the face recognition, we encrypt the gallery set on the cloud. Clients can upload their private data for recognition. For the classification task, we encrypt the data transmitted to the classification model. Experimental results on multiple datasets show that the proposed method is effective. In addition, to prove the effectiveness of our proposed loss, we conduct ablation study about it to further present the advantages of our proposed method.

Our main contributions are as follows:

- Inspired by Type-I adversarial attacks, we propose a visual privacy protection method AVP. To alleviate the difficult trade-off between capability of privacy protection and quality of recovered data, we design a variance consistency loss to better hide visual information.
- Our proposed method has following properties: 1) The visual information of encrypted data and original data is quite different. 2) Our method does not require retraining DNNs. 3) The encrypted data can be recovered by the own key model but is difficult for external models to recover and steal visual information.
- We validate the effectiveness of the proposed method on the face recognition task and the classification task. In addition, we conduct qualitative and quantitative ablation studies to show efficiency of the proposed loss.

2 Related Work

Visual privacy protection. The privacy protection of image visual information is from the perspective of human vision. It is most directly manifested by the fact that the protected images are visually unrecognizable. HE-based

methods which are more secure are mainly derived from cryptography. However, it is usually not suitable for nonlinear computations. And most DNNs contain a large amount of nonlinear computation, so HE-based methods hardly applicable to state-of-the-art DNNs [6]. Therefore, this type of methods is not discussed in this paper. For the PE-based methods, [10, 6, 11, 12] focus their attention on finding an encrypted domain and train the model directly using the encrypted images. However, this has a significant impact on the accuracy of the model and lacks flexibility. To improve the accuracy of the classification model for encrypted images, a transformation network is trained in [13] to keep the classifier correctly classified while encrypting the images. However, a major weakness of this method is that the encrypted image cannot be decrypted.

Unlike the above work used in classification and segmentation tasks, we mainly focus on face recognition which has more emphasis on privacy, and our method can be well generalized to other fields, such as classification tasks. Our proposed method can also compensate for the drawbacks of the above methods. It encrypts the image for a specific model that already exists, and it takes advantage of the vulnerability in the model itself to provide a strong privacy protection to the image. Since our method does not modify the target model, it does not affect the accuracy of the model on the original image.

Adversarial Attack. DNNs are very vulnerable to some adversarial examples [14, 15]. There are many adversarial attack methods [14, 20, 21] being proposed to efficiently find adversarial examples. [19] divided the adversarial attacks into adversarial attack Type-I and adversarial attack Type-II based on the statistical Type I error and Type II error. We take an optimization perspective on adversarial attacks, then the Type-II attack is to maximize the difference in the model output while ensuring that the difference with the original input samples is slight. Mathematically,

$$\max_{x'} f(x) - f(x') \quad s.t. \quad \|x' - x\| < \epsilon \quad . \quad (1)$$

where x is the original sample, x' is the adversarial sample, and $f(\cdot)$ is the model which is attacked. The Type-I attack, in contrast to the Type-II attack, looks for an input sample that differs the most possible from the original input sample, but makes the output of the model consistent. Mathematically,

$$\max_{x'} \|x' - x\| \quad s.t. \quad f(x) = f(x') \quad . \quad (2)$$

The Type-I attack on classification networks and generative adversarial networks was also implemented in [19]. Then, [22] implemented a Type-I attack against variational autoencoder (VAE) [23]. In this work, we implement a Type-I attack on face recognition task and classification task, and propose AVP method based on it.

3 Methodology

The objective of our proposed method is to learn an encrypted image x' which is satisfied that 1) is completely different from the original image x , 2) for the target model the output $f_t(x')$ is the same as the original image $f_t(x)$, and 3) can be recovered as the original image x by the *key* model. Mathematically,

$$\begin{aligned} &\text{From } x \in \mathcal{X} \quad \text{Generate } x' = \mathcal{A}(x) \\ &s.t. \quad \|x' - x\| > \epsilon \\ &\quad f_t(x') = f_t(x), \quad key(x') = x. \end{aligned} \quad (3)$$

The schematic diagram is shown in Fig. 2.

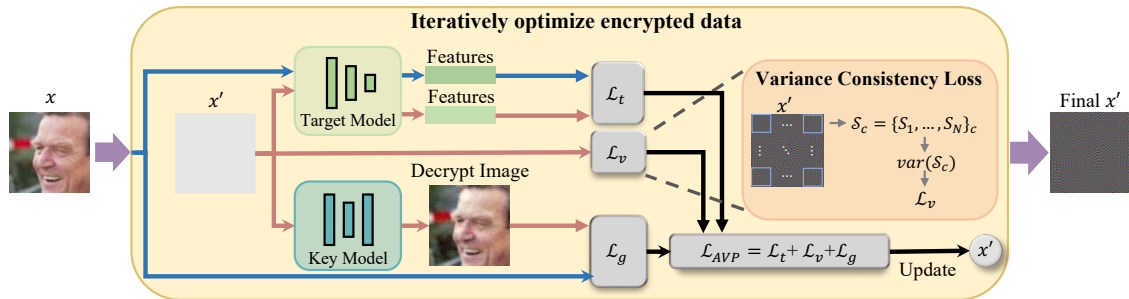


Figure 2: Overview of adversarial attack-based visual privacy protection (AVP) method. Taking the face recognition as an example, given a target model and a pre-trained key model, we encrypt the original data x and obtain the encrypted data x' .

3.1 Image Encryption

Exploiting the adversarial vulnerability of DNNs, we can perform Type-I attack on DNN model to get images that are visually completely different from the original image but with extremely similar features. Suppose that $d(\cdot)$ measures the difference between model outputs, and for different tasks it behaves as a different function. Then for a particular target model f_t , the difference between the output of the adversarial sample and the original sample is

$$\mathcal{L}_t(x', x) = d(f_t(x), f_t(x')). \quad (4)$$

We define \mathcal{L}_d as

$$\mathcal{L}_d(x', x) = \|x - x'\|_2^2, \quad (5)$$

then the loss of the Type-I attack on the target model is as follows:

$$\mathcal{L}_r(x', x) = \mathcal{L}_t(x', x) - \lambda \cdot \mathcal{L}_d(x', x), \quad (6)$$

where λ is a positive hyperparameter which balances image level differences and output level differences. Then with a certain number of iterations K , We can optimize \mathcal{L}_r by the following operations to get the final adversarial sample.

$$g_{k+1} = \alpha \cdot g_k + \frac{\nabla \mathcal{L}(x'_k, x)}{\|\nabla \mathcal{L}(x'_k, x)\|_2}, \quad (7)$$

$$x'_{k+1} = x'_k + \beta \cdot g_{k+1}, \quad (8)$$

where

$$g_0 = \frac{\nabla \mathcal{L}(x'_0, x)}{\|\nabla \mathcal{L}(x'_0, x)\|_2}. \quad (9)$$

At the first iteration, x'_0 can be randomly initialized, or it can be made $x'_0 = x$. The former provides an easier way to get a adversarial example with greater visual differences, while the latter provides a faster way to get a adversarial example that meets the criteria.

3.2 Image Decryption

The image obtained by the loss function of Eq. 6 can provide the effect of privacy protection and can keep its function for the target model. However, the protected image obtained is not recoverable. To achieve the goal of Eq. 3, we attach a decryption module which can recover the generated privacy-protected image. Since the process of generating the privacy-protected image and recovering the privacy-protected image is equivalent to a process of encryption and decryption, we refer to the generated privacy-protected image as an encrypted image and the generation model that can recover the encrypted image as the key model.

To get the encrypted images, we first train the generative model G which can generate the same images as the input. In this work, we use a generative model based on the pix2pix framework. Then we perform Type-I attacks on both the target model and the generative model. We define \mathcal{L}_g as

$$\mathcal{L}_g(x', x) = \|x - G(x')\|_2^2. \quad (10)$$

It can help to keep the encrypted images recoverable by the key model we have chosen. Thus, the loss becomes as follows:

$$\mathcal{L}_e(x', x) = \mathcal{L}_r(x', x) + \mu \mathcal{L}_g(x', x), \quad (11)$$

where μ is a hyperparameter that balances the encryption quality and decryption quality. With Eq. 7 and Eq. 8, we can optimize \mathcal{L}_e to obtain the encrypted image x' , which can satisfy the objective of Eq. 3.

3.3 Variance Consistency Loss

The encrypted image obtained by the objective function of Eq. 6 satisfies the requirements of Eq. 3, but its encryption quality is not high. The obtained encrypted images have the problem of difficult trade-off between encryption quality and decryption quality. That is, if we want to obtain an image that is difficult to be attacked successfully, the quality of the image recovered by the key model will be poor. Another problem is that the obtained encrypted image, although differing greatly from the original in color, exists obvious visual information that the original image has, which has a negative impact on privacy protection. To solve the above problem, we propose a variance consistency loss. It improves

Algorithm 1 Adversarial Attack-based Visual Privacy Protection Method

Input: Target model f_t ; key model G ; original image x ; number of iterations K ; gradient g ; number of times the loss has increased num ; maximum number of times the loss increase $maxnum$.

Output: Encrypted images x' .

```

1:  $g_0 = 0$ ;  $num = 0$ ;
2: Random initialization  $x'_0$ ;
3: for  $k = 0$  to  $K$  do
4:   Compute  $\mathcal{L}_{AVP}(x'_k, x)$  via Eq. 15;
5:    $g_{k+1} = \alpha \cdot g_k + \frac{\nabla \mathcal{L}_{AVP}(x'_k, x)}{\|\nabla \mathcal{L}_{AVP}(x'_k, x)\|_2}$  (Eq. 7);
6:    $x'_{k+1} = x'_k + \beta \cdot g_{k+1}$  (Eq. 8);
7:   if  $\mathcal{L}_{AVP}(x'_{k-1}, x) < \mathcal{L}_{AVP}(x'_k, x)$  then
8:      $num = num + 1$ ;
9:   end if
10:  if  $num > maxnum$  then
11:     $\beta = 0.85\beta$ ;
12:     $num = 0$ ;
13:  end if
14: end for
    
```

the quality of encryption by limiting the differences of each part of the image to make the encrypted image visually more confusing.

For the input image, we divide the data in each channel (R, G, B) into N blocks respectively, *i.e.*, $\{b_1, b_2, \dots, b_N\}_c$, where $c \in \{R, G, B\}$, $b_n \in \mathbb{R}^{h \times w}$ and h, w denote the height and width of the block. The pixels of the blocks are allowed to have overlapping parts between them. Let $p_{i,j}^{b_n} \in [0, 1]$ denote the normalized pixel value at (i, j) in block b_n . Then, we calculate the sum of each block:

$$S_n = \sum_{i=1}^h \sum_{j=1}^w p_{i,j}^{b_n}. \quad (12)$$

We use \mathcal{S} denote the set of sum of the blocks for each channel, *i.e.*, $\mathcal{S}_c = \{S_1, S_2, \dots, S_N\}_c$. In our practice, we convolve the image with a convolution kernel of size $h \times w$ to obtain blocks. Then, we calculate the variance of \mathcal{S}_c and obtain $\sigma_c^2 = \text{var}(\mathcal{S}_c)$. Finally, we define the variance consistency loss as:

$$\mathcal{L}_v(x') = \sigma_R^2 + \sigma_G^2 + \sigma_B^2, \quad (13)$$

where σ_R, σ_G and σ_B denote the variances for R, G, B channels, respectively. By minimizing \mathcal{L}_v , we can get an encrypted image with a more uniform distribution of pixel values. Proof-of-concept experiments (see Sec. 4.4) show that \mathcal{L}_v can eliminate the visual semantics in the encrypted images which are similar to the original images, and can help obtain encrypted images with high quality of encryption and decryption.

Based on the variance consistency loss, the loss function in Eq. 6 is modified as

$$\mathcal{L}_r(x', x) = \mathcal{L}_t(x', x) + \lambda \mathcal{L}_v(x', x), \quad (14)$$

and the Eq. 11 is reformulated as

$$\mathcal{L}_{AVP}(x', x) = \mathcal{L}_t(x', x) + \lambda \mathcal{L}_v(x', x) + \mu \mathcal{L}_g(x', x), \quad (15)$$

where μ are hyperparameters. This is the AVP framework that we propose. The algorithm is summarized in Algorithm 1.

3.4 AVP Method for Specific Tasks

Our proposed AVP method can be applied to a wide range of tasks. In this work, we take the face recognition and the classification as examples to illustrate the ability of AVP.

For the face recognition task, we want the features extracted by the target face recognition model from the encrypted image and the original image to be as same as possible. Thus, we reify \mathcal{L}_t as:

$$\mathcal{L}_t(x', x) = \|f_t(x) - f_t(x')\|_2^2. \quad (16)$$

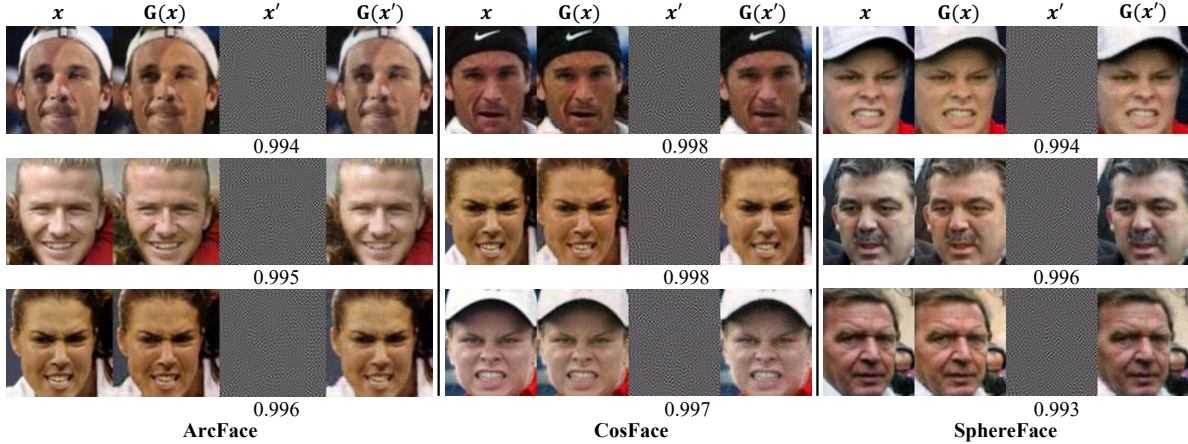


Figure 3: Adversarial attack-based visual privacy protection (AVP) method encrypts face images for different target models. We mark below each encrypted image the cosine similarity between the feature vector of it and the original image.

For the classification task, compared with directly minimizing the mean square error (MSE) of $f_t(x)$ and $f_t(x')$, we find that maximizing $f_t^c(x')$ where c is the prediction class of the target model on the original image can more effectively reduce the impact of encryption on the accuracy. We thus first obtain the logit output of the original image $f_t(x)$ and convert it to one-hot format ($f_t(x)$). Then, we reify \mathcal{L}_t as

$$\mathcal{L}_t(x', x) = -(f_t(x)) \cdot f_t(x'). \quad (17)$$

4 Experiments

In this section, we first verify the effectiveness of the AVP method for face recognition tasks. Then, taking the face recognition system as an example, the security of the AVP method and the effectiveness of the variance consistency loss are explored. Finally, we verify the effectiveness of the AVP method for classification tasks.

4.1 Experimental Settings

Dataset and target models. Our experiments were mainly evaluated based on the *Labeled Face in the Wild (LFW)* [24] dataset. And we choose four face recognition models ArcFace [25], CosFace [26], SphereFace [27] used in [18] and AdaFace [28] to fully evaluate the performance of our method. Among them, the input size of ArcFace and AdaFace [28] is 112×112 , and the input size of CosFace and SphereFace is 112×96 . Therefore, we use the MTCNN [29] to align and crop the face images to the input size of the corresponding face recognition model first.

Key models. We choose the pix2pix framework [30] to train our key model. It has the same structure as the generator used in [31]. To pre-train the key model, we first randomly selected 1,2878 images from the *CelebA* [32] dataset as the training set. Then we set the input and output of the model to the same image, set the batch size to 1, and train 4 epochs. Finally, the trained generator is used directly as the key model.

Evaluation Metrics. To evaluate the effectiveness of our method in a more realistic way and inspired by the evaluation method in [33], we modified the evaluation method of *LFW*. We randomly selected 12 persons from the *LFW* dataset as the probe set, each of them contains more than 12 facial images, for a total of 355 images. For the other 12878 images,

Table 1: $SSIM_e$, $SSIM_d$ and cosine similarity (cos-sim) between original image features and encrypted image features on *LFW*.

	$SSIM_e \downarrow$	$SSIM_d \uparrow$	cos-sim \uparrow
AdaFace	0.028	0.893	0.997
ArcFace	0.030	0.903	0.994
CosFace	0.028	0.899	0.998
SphereFace	0.029	0.906	0.996

Table 2: Accuracy (percentage) of face recognition models for original data and different encrypted data on *LFW*. The results of AVP-ONE and AVP-ALL are expected to be close to the results of Original.

Models	Original	AVP-ONE	AVP-ALL
AdaFace	98.6	98.6	98.6
ArcFace	96.5	96.5	96.5
CosFace	89.4	89.2	89.3
SphereFace	80.3	80.0	80.6

Table 3: The performances of our method when the pre-trained model is based on non-face data (*e.g.*, *COCO*).

Model	AVP-ONE(%)	SSIM _e ↑	SSIM _d ↑
AdaFace	98.6	0.026	0.891
ArcFace	96.5	0.027	0.909
CosFace	89.2	0.031	0.882
SphereFace	79.9	0.031	0.890

we use them as gallery set. In the testing phase, we take one face image of a person in the probe set and put it into the gallery set, and then use the remaining images of this person as the test set. Next, we use the above divided dataset to test the accuracy of the face recognition model. In this way, we put each image of each person in the probe set into the gallery set in turn to measure the total accuracy. This metric can well demonstrate the impact of our method on face recognition models in practical applications.

We use the structural similarity (SSIM) [34] to quantitatively measure the quality of the images. In this work, SSIM_e represents the average of the SSIM values between the encrypted data x' and the original data x , and SSIM_d represents the average of the SSIM values between x and the decrypted data $G(x')$.

4.2 Effectiveness of Face Privacy Protection

Effectiveness and Impact on Target Model. To the best of our knowledge our method is the first (PE)-based methods for face recognition and there is no closely related method yet to compare the performance of encrypted images, so we evaluated both qualitatively and quantitatively on encrypted images. The high recognition accuracy and visual metric scores indicate the validity of our method.

We use the AVP method to encrypt the original face image x^o in the probe set to test its effectiveness on face visual privacy protection. Then, we used the obtained encrypted image x^{en} as the input of the key model $G(\cdot)$ and recovered the encrypted image by $G(x')$ to finally obtain the decrypted image. In addition, we obtained the reconstructed image $G(x)$. The results are shown in Fig. 3. From Fig. 3, it is evident that the encrypted image generated by our method is significantly different from the original image, and no useful visual information is obtained from the encrypted image at all, so it has the effect of visual privacy protection for the original image. In Tab. 1, the average SSIM value between the encrypted image and the original image for each target model is less than 0.04, while the cosine similarity between their features is higher than 0.99. Therefore, the encrypted image generated by AVP can completely replace the original image while protecting the visual information.

To evaluate the impact of our proposed AVP method on the accuracy of the face recognition models, we first generate an encrypted face image in the probe set before putting it into the gallery set, and then put the encrypted image into the gallery set instead of the original image. We tested the accuracy of the face recognition models in this way, and the result AVP-ONE is shown in Tab. 2. Compared with the original accuracy of the models it can be concluded that the impact of the AVP method on image encryption on the accuracy of the models is very slightly which can achieve the same accuracy in the ArcFace model.

Considering the real situation, all the images stored in the gallery set are also encrypted images. So we replaced all the images in the gallery set with encrypted images and then retested the accuracy of the models, as AVP-ALL in Tab. 2. In this case, our method also has a very slightly impact on the accuracy of the models and has a beneficial effect on the accuracy of the SphereFace model.

We test the average of SSIM values, as shown in Tab. 1. Combined with Fig. 3 shows that the decrypted image has good quality and can decrypt most of the visual information of the original image. Since the decrypted images are generated by the generative model, a better trained generative model can achieve better decryption quality.

Randomness of the dataset for training the key model. In this work, we train the key model using the same face image dataset as *CelebA*. However, in real scenarios, large amount face data is often difficult to obtain due to the privacy of each individual involved. So we changed *CelebA* to *COCO* [35] containing various objects to test the effectiveness of

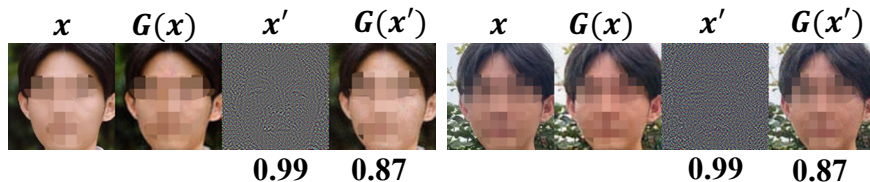


Figure 4: Visual privacy protection in real-world scenes. The cosine similarity between recognition features of encrypted images (x') and original images (x) is marked below x' . SSIM between decrypted images ($G(x')$) and original images is marked below $G(x')$. To maintain anonymity during the submission period, we mosaic the faces.



Figure 5: Partial results of the first security validation experiment. The left column is the key used for encryption, and the top row is the key used for decryption. Every key models are trained with different initialization only. More images of the results are shown in Fig 11 in the Appendix.

the newly key model used to encrypt the data. We choose the test set of *COCO* as the train set, and train 6 epochs on the key model. The results are shown in Tab. 4.2, and it can be concluded that both the impact of encrypted images on the model accuracy and the quality of decrypted images are very slightly different from the key model trained with *CelebA*. Therefore, we can use different types of datasets to train the key model, not just limited to face images.

Real World Face Privacy Protection. We randomly selected real-world face photos taken with phones and then encrypted them to test the performance of the AVP method for using real-world scenarios. Part of results are shown in Fig. 4. In realistic scenarios, the cosine similarity of the features between the encrypted image generated by the AVP method and the original image is still higher than 0.99. And the decrypted image can still be recovered well.

4.3 Security Analysis

Key Model Randomness Analysis. To test the randomness of the key model, we first trained 16 key models consecutively using the same settings but with different initialization values. Different initialization values may result in significantly different trained key models. Then, We choose one of them in turn as the private key model to participate in the encryption of the image, and use the others as the external key model to try to recover the encrypted image. From the results as shown in Fig. 5, it can be concluded that the encrypted data obtained by one private key model cannot be decrypted by other external key models, which demonstrates our proposed method can greatly improves the security of the face visual information. In addition, it is convenient that we can obtain mutually independent keys by simply changing the initialization without changing factors such as the structure of the key model and the training dataset. We suppose that one reason for this phenomenon is due to the instability of GAN training, where different initialization values lead to different locally optimal solutions. Another reason could be that our method tends to find the boundary points of the input field corresponding to the output error allowed by the key model. However, the instability of GAN training causes this boundary to change significantly when the initialization value is changed.

Responding to a Possible Attack. For the key model, even if the key model structure and its training settings are leaked, the encryption is still difficult to break if the initialization point of the key training model is not leaked. As for the data, if pairs of original and encrypted images are leaked in large quantities, then an attacker can directly use these data to train a generative model to directly map the encrypted domain to the original domain. This case is exploited in [36] to evaluate the robustness of encryption. So, we encrypt all the face images in the gallery set using the same key model, producing pairs of encrypted and original images. Then we use these paired images as a training set, and train a model using the same structure as the attack model. Using such a model, we attempt to recover the encrypted images in



Figure 6: Crack the encrypted image using the attack model. The training dataset for the attack model is obtained using key1 encryption. An attacker can recover images encrypted with his own key (key1), but cannot decrypt images encrypted with other keys.

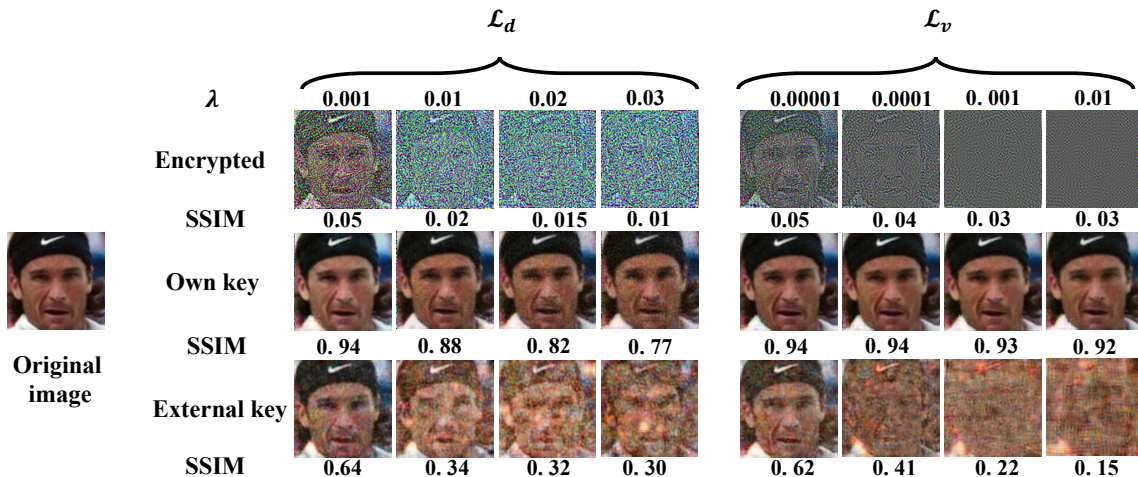


Figure 7: Results of the ablation study. The SSIM values with the original images are shown under each image.

the probe set. The results are shown in Fig. 6. When the training set images and the encrypted image to be cracked are encrypted from the same key model, the attack model can recover the encrypted image. However, when they are encrypted with different key models, the trained model cannot crack the encrypted image. Therefore, we can increase the frequency of changing key models to effectively defend against such attacks.

The encrypted images obtained by our method also have good statistical properties, and the correlation analysis and histogram analysis are shown in Sec. A.1 of the Appendix.

4.4 Ablation Study

We compare the distance loss \mathcal{L}_d with the variance consistency loss \mathcal{L}_v to verify the effectiveness of \mathcal{L}_v . For each loss we choose a set of suitable weights λ separately to represent its trade-off between the encryption quality and decryption quality. Its results are shown in Fig. 7. The encrypted image generated using \mathcal{L}_d has a smaller SSIM value compared to the encrypted image using \mathcal{L}_v , but a clear outline can be seen. So the visual information of the original image still exists. And if the encrypted image is to be made free of such visual information, there is a significant loss in the quality of the decrypted image. In contrast, using \mathcal{L}_v , it is possible to generate encrypted images with both no residual visual information and high decryption quality. We also use another key to decrypt the encrypted image to further investigate the effect of the two different losses on the encryption quality. From Fig. 7, it can be concluded that the encrypted image using \mathcal{L}_v is more difficult to be decrypted by similar key models with different initialization while ensuring the quality of the decrypted image.

4.5 Privacy protection for classification models.

We trained ResNet50 [37], VGG19 [38] using the train set of *CIFAR-10* [39] and implemented AVP method for the images of the test set. The results are shown in Fig. 8. We also compared the two existing privacy protection methods and the results are shown in Tab. 4.4, where [13] do not recover encrypted images. We show the figure of encryption results of the two compared methods and their SSIM values in Sec. A.2 of the Appendix. Our method has minimal impact on the accuracy of the models, and the average SSIM value of the decrypted images can reach above 0.9 for both models after our tests. So, our method can also be applied to classification tasks with good results.

Table 4: Impact of privacy protection methods on the accuracy (percentage) of classification models on *CIFAR-10*.

Method	Model	Original	Encrypt
[10]	VGG19	10.59	87.78
	Resnet50	11.00	91.53
[13]	VGG19	93.95	90.70
	Resnet50	95.53	90.16
AVP	VGG19	93.95	93.95
	Resnet50	95.53	95.28

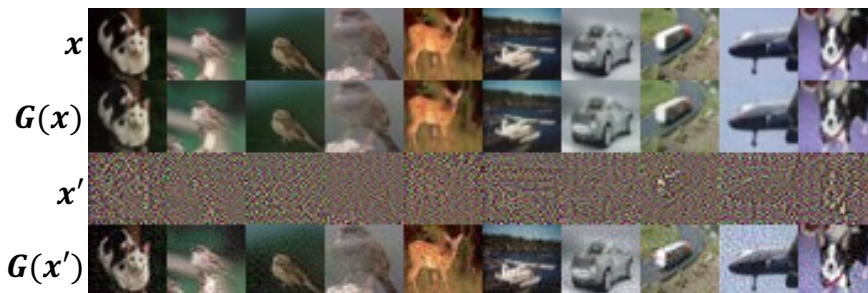


Figure 8: Results of AVP method for Resnet50 as the target model. Each column represents a different sample.

5 Conclusion

In this paper, we propose a visual privacy protection method AVP based on Type-I attack. We evaluate our method by data protection of face recognition system in cloud. Experiments show that the AVP method can encrypt images while preserving their functionality for the target model. We also propose a variance consistency loss to solve the problem of difficult trade-off between encryption quality and decryption quality in the encryption process. Finally, we also using AVP method in classification tasks with satisfactory results. Our work has beneficial effects on the adversarial learning community and the private protection community, even if it also has some drawbacks. We may not discuss and compare private protection methods in detail in this work because we want to explore whether adversarial attacks can be used to hide visual information and provide a new perspective on privacy protection.

References

- [1] L Arockiam and S Monikandan. Efficient cloud storage confidentiality to ensure data security. In *2014 International Conference on Computer Communication and Informatics*, pages 1–5. IEEE, 2014.
- [2] Ashish Singh and Kakali Chatterjee. Cloud security issues and challenges: A survey. *Journal of Network and Computer Applications*, 79:88–115, 2017.
- [3] Seny Kamara and Kristin Lauter. Cryptographic cloud storage. In *International Conference on Financial Cryptography and Data Security*, pages 136–149. Springer, 2010.
- [4] Deyan Chen and Hong Zhao. Data security and privacy protection issues in cloud computing. In *2012 International Conference on Computer Science and Electronics Engineering*, volume 1, pages 647–651. IEEE, 2012.
- [5] Siani Pearson and Azzedine Benameur. Privacy, security and trust issues arising from cloud computing. In *2010 IEEE Second International Conference on Cloud Computing Technology and Science*, pages 693–702. IEEE, 2010.
- [6] Warit Sirichotedumrong, Takahiro Maekawa, Yuma Kinoshita, and Hitoshi Kiya. Privacy-preserving deep neural networks with pixel-based image encryption considering data augmentation in the encrypted domain. In *2019 IEEE International Conference on Image Processing (ICIP)*, pages 674–678. IEEE, 2019.
- [7] Yoshinori Aono, Takuya Hayashi, Lihua Wang, Shiho Moriai, et al. Privacy-preserving deep learning via additively homomorphic encryption. *IEEE Transactions on Information Forensics and Security*, 13(5):1333–1345, 2017.
- [8] Yizhi Wang, Jun Lin, and Zhongfeng Wang. An efficient convolution core architecture for privacy-preserving deep learning. In *2018 IEEE International Symposium on Circuits and Systems (ISCAS)*, pages 1–5. IEEE, 2018.
- [9] Qian Lou and Lei Jiang. She: A fast and accurate deep neural network for encrypted data. *Advances in Neural Information Processing Systems*, 32, 2019.

- [10] Masayuki Tanaka. Learnable image encryption. In *2018 IEEE International Conference on Consumer Electronics-Taiwan (ICCE-TW)*, pages 1–2, 2018.
- [11] Warit Sirichotedumrong and Hitoshi Kiya. A gan-based image transformation scheme for privacy-preserving deep neural networks. In *2020 28th European Signal Processing Conference (EUSIPCO)*, pages 745–749. IEEE, 2021.
- [12] Yi Ding, Guozheng Wu, Dajiang Chen, Ning Zhang, Linpeng Gong, Mingsheng Cao, and Zhiguang Qin. Deepedn: a deep-learning-based image encryption and decryption network for internet of medical things. *IEEE Internet of Things Journal*, 8(3):1504–1518, 2020.
- [13] Hiroki Ito, Yuma Kinoshita, Maungmaung Aprilpyone, and Hitoshi Kiya. Image to perturbation: An image transformation network for generating visually protected images for privacy-preserving deep neural networks. *IEEE Access*, 9:64629–64638, 2021.
- [14] Ian J Goodfellow, Jonathon Shlens, and Christian Szegedy. Explaining and harnessing adversarial examples. *arXiv preprint arXiv:1412.6572*, 2014.
- [15] Andrew Ilyas, Shibani Santurkar, Dimitris Tsipras, Logan Engstrom, Brandon Tran, and Aleksander Madry. Adversarial examples are not bugs, they are features. *Advances in neural information processing systems*, 32, 2019.
- [16] Mahmood Sharif, Sruti Bhagavatula, Lujo Bauer, and Michael K Reiter. Accessorize to a crime: Real and stealthy attacks on state-of-the-art face recognition. In *Proceedings of the 2016 acm sigsac conference on computer and communications security*, pages 1528–1540, 2016.
- [17] Seong Joon Oh, Mario Fritz, and Bernt Schiele. Adversarial image perturbation for privacy protection a game theory perspective. In *2017 IEEE International Conference on Computer Vision (ICCV)*, pages 1491–1500. IEEE, 2017.
- [18] Xiao Yang, Yinpeng Dong, Tianyu Pang, Hang Su, Jun Zhu, Yuefeng Chen, and Hui Xue. Towards face encryption by generating adversarial identity masks. In *Proceedings of the IEEE/CVF International Conference on Computer Vision*, pages 3897–3907, 2021.
- [19] Sanli Tang, Xiaolin Huang, Mingjian Chen, Chengjin Sun, and Jie Yang. Adversarial attack type i: Cheat classifiers by significant changes. *IEEE transactions on pattern analysis and machine intelligence*, 43(3):1100–1109, 2019.
- [20] Seyed-Mohsen Moosavi-Dezfooli, Alhussein Fawzi, and Pascal Frossard. Deepfool: a simple and accurate method to fool deep neural networks. In *Proceedings of the IEEE conference on computer vision and pattern recognition*, pages 2574–2582, 2016.
- [21] Francesco Croce and Matthias Hein. Reliable evaluation of adversarial robustness with an ensemble of diverse parameter-free attacks. In *International conference on machine learning*, pages 2206–2216. PMLR, 2020.
- [22] Chengjin Sun, Sizhe Chen, Jia Cai, and Xiaolin Huang. Type i attack for generative models. In *2020 IEEE International Conference on Image Processing (ICIP)*, pages 593–597. IEEE, 2020.
- [23] Diederik P Kingma and Max Welling. Auto-encoding variational bayes. *arXiv preprint arXiv:1312.6114*, 2013.
- [24] Gary B Huang, Marwan Mattar, Tamara Berg, and Eric Learned-Miller. Labeled faces in the wild: A database for studying face recognition in unconstrained environments. In *Workshop on faces in 'Real-Life' Images: detection, alignment, and recognition*, 2008.
- [25] Jiankang Deng, Jia Guo, Niannan Xue, and Stefanos Zafeiriou. Arcface: Additive angular margin loss for deep face recognition. In *Proceedings of the IEEE/CVF conference on computer vision and pattern recognition*, pages 4690–4699, 2019.
- [26] Hao Wang, Yitong Wang, Zheng Zhou, Xing Ji, Dihong Gong, Jingchao Zhou, Zhifeng Li, and Wei Liu. Cosface: Large margin cosine loss for deep face recognition. In *Proceedings of the IEEE conference on computer vision and pattern recognition*, pages 5265–5274, 2018.
- [27] Weiyang Liu, Yandong Wen, Zhiding Yu, Ming Li, Bhiksha Raj, and Le Song. Spheroface: Deep hypersphere embedding for face recognition. In *Proceedings of the IEEE conference on computer vision and pattern recognition*, pages 212–220, 2017.
- [28] Minchul Kim, Anil K Jain, and Xiaoming Liu. Adaface: Quality adaptive margin for face recognition. In *Proceedings of the IEEE/CVF Conference on Computer Vision and Pattern Recognition*, pages 18750–18759, 2022.
- [29] Kaipeng Zhang, Zhanpeng Zhang, Zhifeng Li, and Yu Qiao. Joint face detection and alignment using multitask cascaded convolutional networks. *IEEE signal processing letters*, 23(10):1499–1503, 2016.

- [30] Phillip Isola, Jun-Yan Zhu, Tinghui Zhou, and Alexei A Efros. Image-to-image translation with conditional adversarial networks. In *Proceedings of the IEEE conference on computer vision and pattern recognition*, pages 1125–1134, 2017.
- [31] Jun-Yan Zhu, Taesung Park, Phillip Isola, and Alexei A Efros. Unpaired image-to-image translation using cycle-consistent adversarial networks. In *Proceedings of the IEEE international conference on computer vision*, pages 2223–2232, 2017.
- [32] Ziwei Liu, Ping Luo, Xiaogang Wang, and Xiaoou Tang. Deep learning face attributes in the wild. In *Proceedings of the IEEE international conference on computer vision*, pages 3730–3738, 2015.
- [33] Ira Kemelmacher-Shlizerman, Steven M Seitz, Daniel Miller, and Evan Brossard. The megaface benchmark: 1 million faces for recognition at scale. In *Proceedings of the IEEE conference on computer vision and pattern recognition*, pages 4873–4882, 2016.
- [34] Zhou Wang, Alan C Bovik, Hamid R Sheikh, and Eero P Simoncelli. Image quality assessment: from error visibility to structural similarity. *IEEE transactions on image processing*, 13(4):600–612, 2004.
- [35] Tsung-Yi Lin, Michael Maire, Serge Belongie, James Hays, Pietro Perona, Deva Ramanan, Piotr Dollár, and C Lawrence Zitnick. Microsoft coco: Common objects in context. In *European conference on computer vision*, pages 740–755. Springer, 2014.
- [36] Hiroki Ito, Yuma Kinoshita, and Hitoshi Kiya. Image transformation network for privacy-preserving deep neural networks and its security evaluation. In *2020 IEEE 9th Global Conference on Consumer Electronics (GCCE)*, pages 822–825. IEEE, 2020.
- [37] Kaiming He, Xiangyu Zhang, Shaoqing Ren, and Jian Sun. Deep residual learning for image recognition. In *Proceedings of the IEEE conference on computer vision and pattern recognition*, pages 770–778, 2016.
- [38] Karen Simonyan and Andrew Zisserman. Very deep convolutional networks for large-scale image recognition. *arXiv preprint arXiv:1409.1556*, 2014.
- [39] Alex Krizhevsky, Geoffrey Hinton, et al. Learning multiple layers of features from tiny images. 2009.
- [40] Hossein Movafegh Ghadirli, Ali Nodehi, and Rasul Enayatifar. An overview of encryption algorithms in color images. *Signal Processing*, 164:163–185, 2019.
- [41] Aqeel ur Rehman, Xiaofeng Liao, Rehan Ashraf, Saleem Ullah, and Hueiwei Wang. A color image encryption technique using exclusive-or with dna complementary rules based on chaos theory and sha-2. *Optik*, 159:348–367, 2018.

A Appendix

A.1 Security Analysis

A.1.1 Key Model Space Analysis:

In our proposed method, we choose the generative model as the key, which has a large key space. Take the key model used in our experiments as an example, it has a size of 11.383M. Such a large key space can be disastrous for those who use exhaustive attacks.

A.1.2 Histogram Analysis and Correlation Analysis:

Plain images have a strong correlation between two adjacent pixels in the horizontal and vertical directions[40], and encryption methods with good properties often need to break this correlation[41]. Therefore, we performed a correlation analysis of our proposed method, and its results are shown in Fig. 9. Compared to the strong correlation of the original image, the encrypted image we obtained greatly reduces the correlation between adjacent pixels. We also performed histogram analysis on the original and encrypted images, and the results are shown in Fig. 10. From it, it can be concluded that the histogram statistical properties of the encrypted image and the original image are completely different, and the encrypted image more closely resembles a gaussian distribution. So the encrypted images obtained by AVP method have well statistically characteristics.

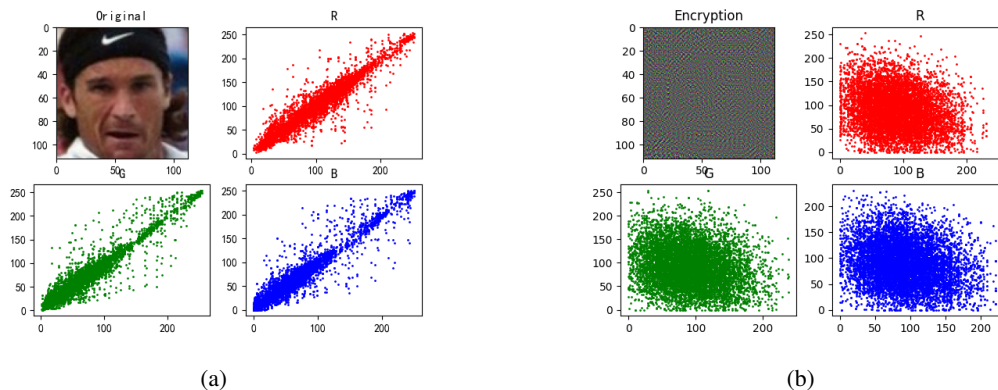


Figure 9: Results of correlation analysis. We randomly select 3000 pairs of adjacent pixel points for the original and encrypted images, respectively, and calculate their correlation coefficients in horizontal, vertical and diagonal directions. (a) and (b) are the results of the original image and the encrypted image, respectively.

Table 5: Impact of privacy protection methods on the accuracy (percentage) of classification models on *CIFAR-10*.

Method	Model	SSIM _e	SSIM _d
[10]	VGG19	0.178	1.000
	Resnet50	0.178	1.000
[13]	VGG19	0.068	-
	Resnet50	0.073	-
AVP	VGG19	0.171	0.900
	Resnet50	0.198	0.923

A.2 Privacy Protection for Classification Tasks

A.2.1 Detailed experimental setup:

When implementing the AVP method on the classification task, we adjust the batchsize to 10 and initialize the encrypted image as the original image. Also we set the number of iterations to 600.

A.2.2 The Quality of Decrypted Images:

We show the encryption results of both methods [10] and [13] in Fig 12. We tested the average SSIM values of the AVP method for the encrypted and decrypted images of the test set in *CIFAR-10* [39]. The results are shown in Table 5. We compare our results with [10] and [13], where [10] recovers the original image, but the encryption quality is weaker and has a significant impact on the model accuracy. [13] mitigates the impact of the encrypted image on the model accuracy, but the encrypted image becomes unrecoverable. And our method ensures a strong encryption strength while the impact on the model accuracy is very slight.

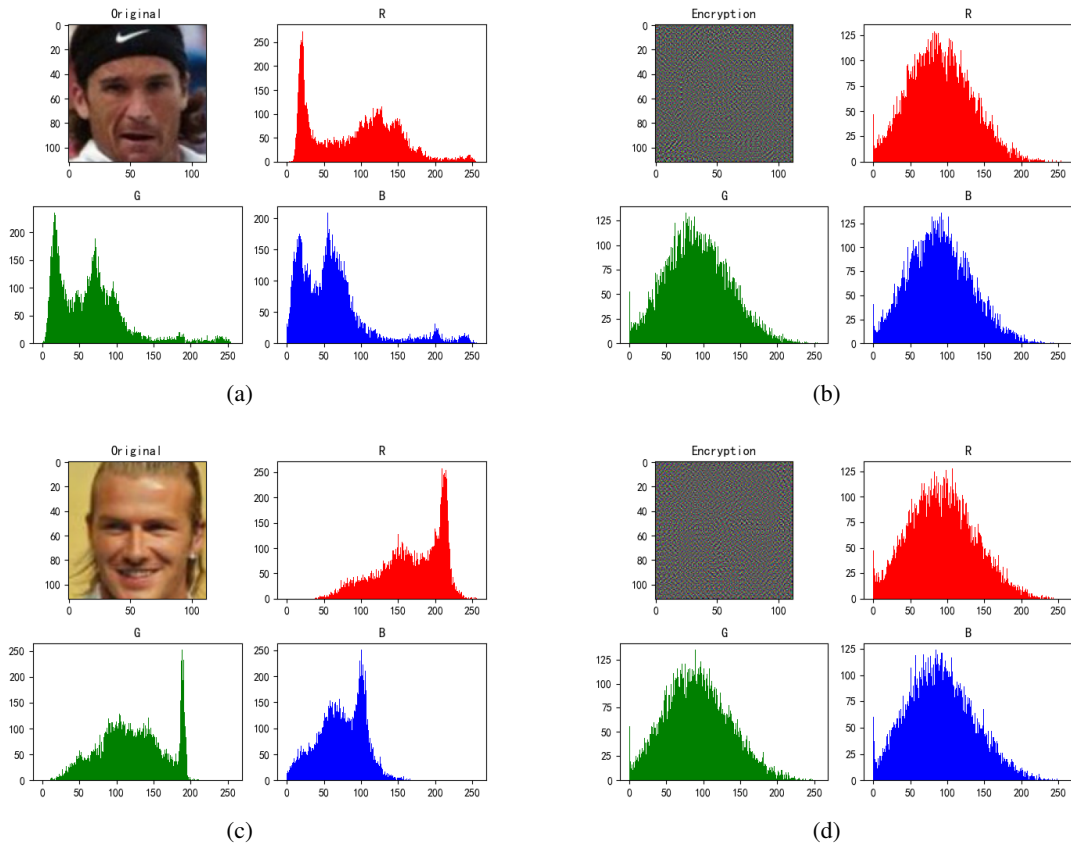


Figure 10: Results of histogram analysis of some original and encrypted images. (a) and (c) are the original images, and (b) and (d) are the encrypted images of them, respectively.

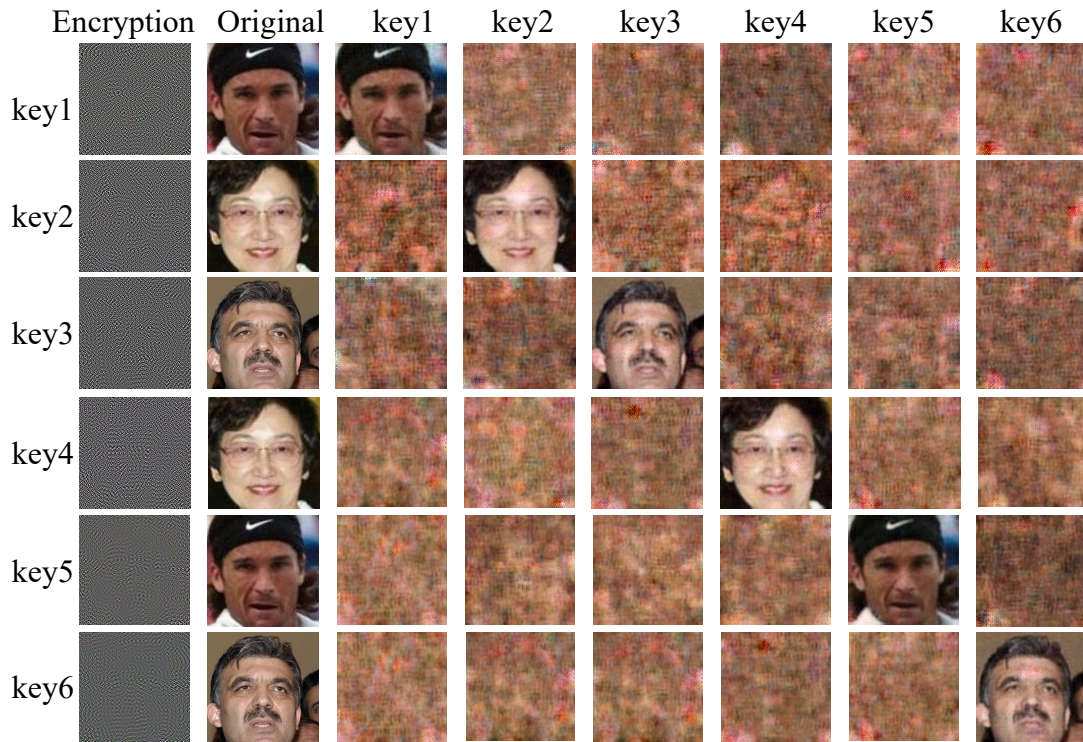


Figure 11: Results of the key model randomness analysis. Due to space limitations, we show the results for 6 key models.



Figure 12: The results of the methods in [10, 13]. (a) is the method in [10], and (b) is the method in [13]. Each column represents a different sample.